J. Physiol. (1983), **345**, *pp.* 533–548
With 8 text-figures
Printed in Great Britain

CALCIUM TAIL CURRENTS IN VOLTAGE-CLAMPED INTACT NERVE CELL BODIES OF *APLYSIA CALIFORNICA*

BY ROGER ECKERT* AND DOUGLAS EWALD

From the Department of Biology and Ahmanson Laboratory of Neurobiology, University of California, Los Angeles, CA 90024, and Friday Harbor Laboratories, Friday Harbor, WA, U.S.A.*

(*Received 22 February 1983*)

SUMMARY

1. Calcium tail currents were measured in axotomized *Aplysia* neurones L2–L6 using a two-electrode voltage clamp and micro-electrodes of specially low resistance. Measurements were made at −40 mV following depolarizing pulses of 7 or 10 ms duration in the presence of 45 μM-tetrodotoxin and 200 mM-tetraethylammonium.

2. Symmetrical currents were eliminated by addition of digitally stored current traces produced in response to equivalent hyperpolarizations. The remaining current, identified as a tail current, was blocked by replacement of extracellular calcium with cobalt or manganese.

3. Computer fits showed that the tail current closely approximated the sum of two exponentially decaying components. The first had a time constant, τ_1, of $0{\cdot}38 \pm 0{\cdot}05$ ms, which may have been frequency-limited by the speed of the clamp; the second had a time constant, τ_2, of $2{\cdot}0 \pm 0{\cdot}8$ ms. A more slowly decaying third tail current component ($\tau_3 = 30$ ms), which developed more slowly, may be related to the non-specific current rather than the calcium current.

4. The τ_1 and τ_2 components of the tail current lost amplitude with increasing pulse duration along an approximately bi-exponential time course that resembled the time course of relaxation of the calcium current during a prolonged depolarization. The slow third component of the tail current showed no such inactivation.

5. The amplitudes of the first and second components of the calcium tail current both increased as sigmoidal functions of the test pulse voltage, reaching half maximum at +20 mV and plateauing above +60 mV. The voltage dependencies of the two components were similar.

6. The rate of decay of the τ_1 component increased with increasing temperature and with increasing negative potential, whereas τ_2 showed little dependence on these parameters.

7. The rates of decay of neither the τ_1 nor the τ_2 component were affected by large changes in the amplitude of the test depolarization or in the amplitude of the tail current or by injection of calcium ions or EGTA. Thus, the kinetics of the tail current as resolved under our conditions appear to be virtually independent of calcium-mediated inactivation.

* Address for reprint requests.

8. Activation time constants (τ_m) predicted from τ_1 are 3 to 5 times longer than the values of τ_m determined from the half-time to peak of activation. These kinetics are slower than those reported for *Limnaea* by factors of 2·5 to 3·5. This can be attributed primarily to differences in experimental temperature and perhaps to some extent to differing frequency limitations of the recording methods.

9. It is suggested that the τ_1 and τ_2 components of the tail current reflect the multistate kinetics of a single class of calcium channels.

INTRODUCTION

Ion channels activated by membrane depolarization exhibit time-dependent deactivation in response to repolarization, presumably because the gating mechanism relaxes to its closed 'resting' state upon removal of depolarization. Individual open channels continue to carry current following repolarization until they close, giving rise to a 'tail current', the time course of which is believed to reflect the kinetics of the closing process(es). Tail currents were first recorded by Hodgkin & Huxley (1952*a*) to determine instantaneous current–voltage relations of the sodium conductance in the space- and voltage-clamped squid giant axon, using low-impedance axial wire electrodes. More recently, the dialysed cell preparation (Kostyuk, Krishtal & Pidoplichko, 1975; Lee, Akaike & Brown, 1978; Byerly & Hagiwara, 1982) has permitted tail current measurements from neurone cell bodies by means of low-impedance access for current delivery through the perfusion pipette. However, cell dialysis presents certain limitations for physiological studies. The procedure removes small molecules from the cell interior, disturbing metabolism and normal intracellular calcium buffering, thus necessitating the use of EGTA or other means of artificially buffering intracellular free calcium ions. There also appears to be a progressive decline of the calcium current in dialysed cells, perhaps due to 'wash-out' of molecules essential for maintenance of the calcium channels (Byerly & Hagiwara, 1982).

Because of their inherent noise and frequency limitations, micro-electrodes provide a less satisfactory mean of voltage clamping the cell for measurement of tail currents; on the other hand, they are less intrusive than the cell perfusion technique, and are thus preferable for certain studies that require minimal disturbance of normal calcium metabolism. A case in point is the characterization of calcium-mediated inactivation of the calcium current (Brehm & Eckert, 1978; Tillotson, 1979; Ashcroft & Stanfield, 1981, 1982; Eckert, 1981; Eckert & Ewald, 1981, 1983; Eckert & Tillotson, 1981; Eckert, Tillotson & Brehm, 1981; Plant & Standen, 1981), a process in which the normal calcium buffering of the cell plays a key role. To this end, we have measured calcium tail currents in intact neurones of *Aplysia californica* using a conventional two-electrode voltage clamp with micro-electrodes of specially low resistance. We were able to recognize three components of decay in the tail currents recorded in these neurones. The first two components appear to arise from deactivation of the calcium channels, with both components exhibiting similar conductance–voltage relations, but differing in certain other respects. The third and slowest component is of uncertain origin.

METHODS

The abdominal ganglion of *Aplysia californica* (Marine Specimens Unlimited, Pacific Palisades, Ca) was placed for 15–20 min in a 1 % solution of Protease Type V (Sigma) dissolved in sea water to facilitate gentle removal of the connective tissue sheath. A transverse cut was made through the left hemiganglion just below cells L2–L6 so as to axotomize these cells. Axotomy eliminated uncontrolled axon currents and reduced significantly the current transients associated with voltage steps.

The cells were voltage clamped with a two-electrode system in which the current electrode was shielded to within 50 μm of the tip with silver conductive paint (GC Electronics) connected to earth and insulated with a layer of carbowax dissolved in carbon tetrachloride. The current electrodes were filled with 10 M-caesium chloride for high conductivity, and had resistances of 0·2–0·8 MΩ. Voltage electrodes, filled with 3 M-potassium chloride, had resistances of 0·7–1·5 MΩ. Membrane potentials were recorded differentially against an external 3 M-potassium chloride/agar electrode positioned near the ganglion. Series resistance compensation was omitted for the sake of clamp stability; the series resistance was characteristically below 2 kΩ. Current was measured with an operational amplifier in a virtual ground configuration with its summing junction connected to a silver/silver chloride pellet in the bath. Signals were typically digitized at 50 kHz, and were stored on diskette for subsequent processing on a Digital Equipment Corporation 11–23-based computer. Currents in response to equivalent depolarizing and hyperpolarizing pulses were added before processing to cancel symmetrical leakage and capacitive currents. For pulses exceeding 60 mV, the hyperpolarization was delivered twice at half amplitude to minimize distortions due to non-linearity.

Sodium current was greatly reduced by axotomy, and the remaining sodium current was blocked with 45 μM-tetrodotoxin (TTX). Potassium currents were suppressed with 200 mM-extracellular tetraethylammonium (TEA) chloride (Eastman, Rochester, NY) replacing an equal amount of sodium chloride. At +20 mV this concentration of TEA reduces the voltage-dependent potassium current, $I_{K(V)}$, to less than 10 % of normal, and the calcium-dependent current, $I_{K(Ca)}$, to less than 1 % of normal. At −40 mV (the potential at which tail currents were measured) $I_{K(Ca)}$ is reduced to the order of one nanoampere by extracellular TEA (Hermann & Gorman, 1981*a*). The 1 M-TEA chloride stock solution was extracted with ethyl ether to remove contaminant triethylamine that can alkalize the cell (Zucker, 1981). Experiments were performed at 12·5–14 °C, except as specified otherwise, with temperature regulated during each experiment to within ±0·3 °C. These temperatures were low enough to slow the tail currents to a readily measured rate of decay without excessive reduction of their amplitudes, and are close to the temperatures experienced by the animals in their environment.

Test pulses of 7 or 10 ms were used because these durations were long enough to activate a significant fraction of the calcium channel population, and short enough to minimize intracellular accumulation of calcium ions during the test pulse. Test solutions (Table 1) contained ×2 normal potassium to reduce the difference between the potassium equilibrium potential and the holding potential, V_h. The calcium concentration was raised to ×2 normal to increase the calcium current. A holding potential of −40 mV was used throughout to inactivate the transient outward current, $I_{K(A)}$ (Hagiwara & Saito, 1959; Connor & Stevens, 1971; Hermann & Gorman, 1981*b*).

Computer-assisted analyses of the tail currents were carried out with the following procedure after subtraction of linear symmetrical currents by the '$d+h$' method described in the next section. First, the base-line current level was established as the mean of 96 data points (sample rate, 50 kHz) taken immediately before the test pulse. The inward (negative) tail current following the end of the test pulse (zero time) was subtracted from the base line to give positive values referred to below as 'tail current data'. The data were then displayed logarithmically against time. A time period was selected beginning somewhat past the transition of fast to slow component (generally at about 2 ms after repolarization) and extending to a point 2 ms later, and this segment of data was used for a least-squares regression, which gave the time constant, τ_2, of the slow phase. This slow exponential was extrapolated back to zero time and subtracted from the full tail current data. The difference current was plotted semilogarithmically against time, and data extending over more than a decade were again used for least-squares regression analysis to give the time constant, τ_1, of the initial fast phase. The two extracted exponentials were then summed to synthesize the bi-exponential function which was graphically compared with the recorded tail current data. This method produced a close match between the synthesized bi-exponential and the recorded tail current. The accuracy of this

approach depends on the degree of contamination of the slow phase by the fast component and by signal noise. The amplitudes of the τ_1 and the τ_2 phases of the tail current were taken from the fitted lines. This algorithm was tested on computer-generated double exponentials. The time constants and relative amplitudes of the two components of these artificial tail currents were obtained from a sequence of random numbers in the same range as the actual tail currents. In the ten single-blind trials the program operator extracted values for τ_1 and τ_2 which deviated from the values used to generate the double exponentials by $-4{\cdot}1 \pm 2{\cdot}5\,\%$ and $-5{\cdot}3 \pm 2{\cdot}9\,\%$ (S.D.), respectively. The systematic small underestimations are presumed to arise from the practice of applying a linear least-squares fit to an exponential that is plotted semilogarithmically. The extracted values for the amplitudes of the τ_1 and τ_2 components, measured at 400 μs, deviated by $+0{\cdot}9 \pm 1{\cdot}8\,\%$ and $+12{\cdot}0 \pm 10{\cdot}5\,\%$, respectively.

TABLE 1. Solutions. All artificial sea water (ASW) solutions contained 20 mM-KCl, 45 mM-$MgCl_2$, 0·045 mM-TTX, 10 mM-glucose, 15 mM-Tris adjusted to pH 7·8 with HCl, and the following concentrations of other ions (mM)

		NaCl	$CaCl_2$	TEA-Cl	$CoCl_2$
ASW		468	20	0	0
200 TEA	ASW	268	20	200	0
0 Ca/20 Co	ASW	268	0	200	20

In the case of stimulus pulses exceeding 7–10 ms, there was a measurable third component of decay in the tail current. In such instances a similar curve-stripping procedure was utilized by which τ_1 and τ_2 were evaluated on the basis that $\tau_3 \gg \tau_2 > \tau_1$, so that the amplitude of τ_3 could be regarded as an offset at short times. In such cases, the amplitude of the third current component was subtracted so as to minimize the variance between extrapolated fit and the tail current data.

RESULTS

General description of the calcium tail current

On stepping back from a depolarized level to the holding potential, the voltage-dependent conductance responsible for the inward current seen during the depolarization undergoes deactivation along a time course that produces the tail current. To separate the ionic current during the course of deactivation from the symmetrical capacitive current, the latter was subtracted from the total current by digital summation of the currents elicited with identical depolarizing (*d*) and hyperpolarizing (*h*) test pulses (Fig. 1 *A* and *B*). The ionic tail currents (trace $d+h$) were routinely isolated in this manner.

The early portions of the tail currents were always distorted, exhibiting a characteristic 'hook' during the initial 0·2–0·4 ms after termination of the 60 mV test pulse. This hook may result from imperfect voltage control. In Fig. 1 *C* the capacitive current following a hyperpolarization can be seen to decay with a time constant, τ_C, of 0·08 ms. By 0·4 ms the capacitive current was below 0·1 μA, while the total current was below 1·0 μA. The series resistance in these cells is typically below 2 kΩ, so an error of as much as 2 mV is estimated for the actual membrane potential at that point in time, even though the potential recorded at the electrode tip during the capacitive current was flat within less than 1 mV. The convergence, in time, of (i) increasing driving force on calcium ions, and (ii) increasing deactivation of calcium channels during membrane repolarization may explain the initial hook distorting the current tail. The hooked portion was avoided in our measurements, as described below.

Since the settling time of the actual membrane potential was undoubtedly slower

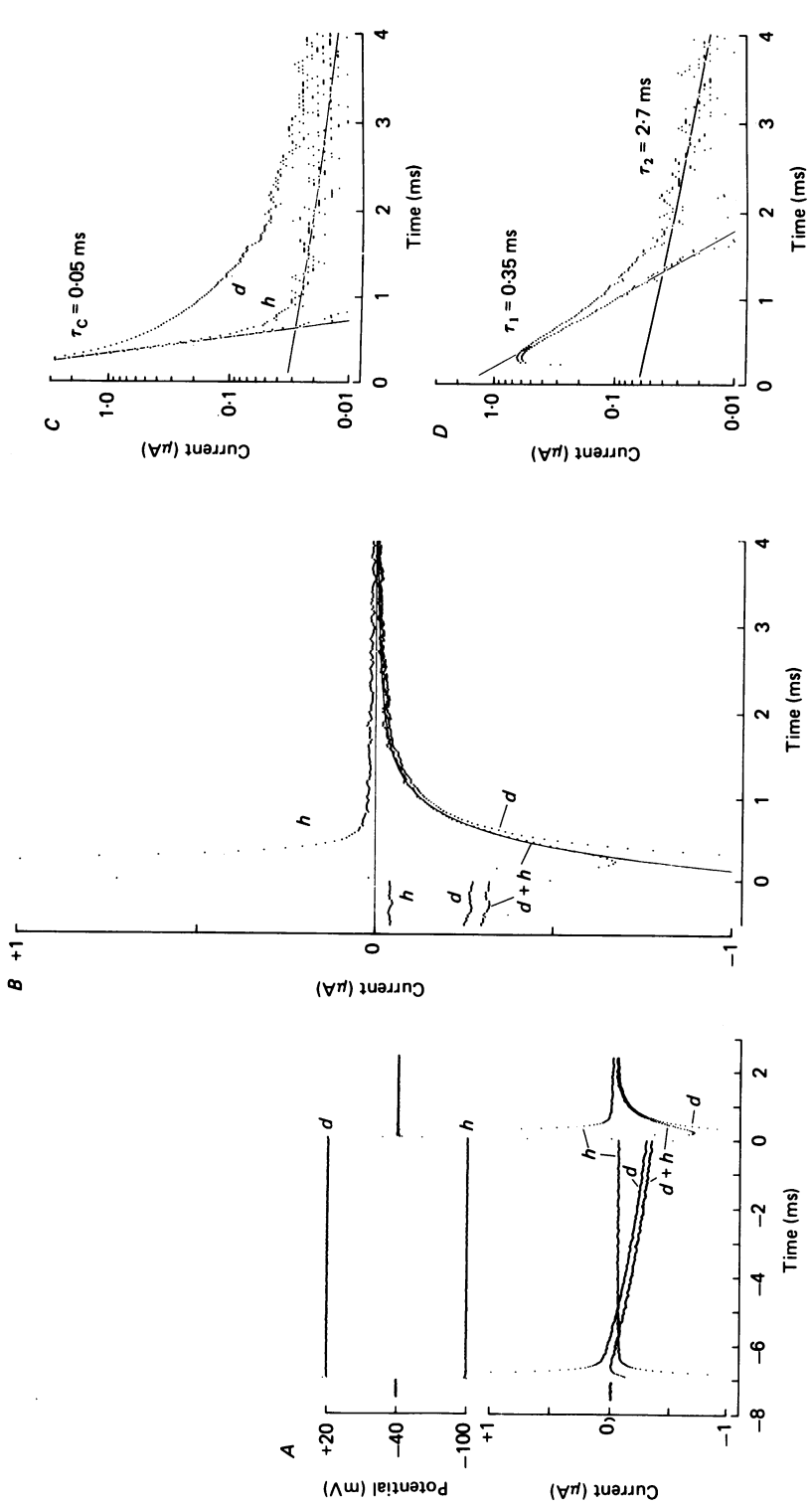

Fig. 1. Method of obtaining the tail current measurements. *A*, a 7 ms (in some cases 10 ms) test pulse was delivered first as a depolarization (d) and then as a hyperpolarization (h). The corresponding membrane currents were stored and digitally summed ($d+h$) to eliminate symmetrical components. *B*, same currents displayed on a larger scale showing a computer-generated continuous trace consisting of one slow and one fast exponential component fitted to the net tail current ($d+h$). *C*, semi-logarithmic displays of the unsummed current transients. The component with the fastest time constant, τ_C, recorded at the termination of the hyperpolarizing pulse (h) is presumed to be the capacitive transient. Plot d is the semilogarithmic display of the uncorrected current having the same label in panel *B*. *D*, semilogarithmic display of the net tail current ($d+h$). The initial fast component, τ_1, was obtained by computer-assisted subtraction of the slower second time constant, τ_2. Both τ_1 and τ_2 were significantly longer than τ_C.

than the potential seen at the recording electrode, backward extrapolation of the exponential decay of the current to the termination of the pulse (i.e. onset of repolarization) would lead to an over-estimation of the instantaneous conductance. Because of this, we made no attempts to extrapolate, but measured the tail current amplitudes at a fixed time (usually 400 μs) following the end of the pulse. By this time the hooked portion was over, and the series resistance error was trivial. The amplitude of the current measured at this time was considered proportional to the calcium conductance present at the instant the test pulse was terminated.

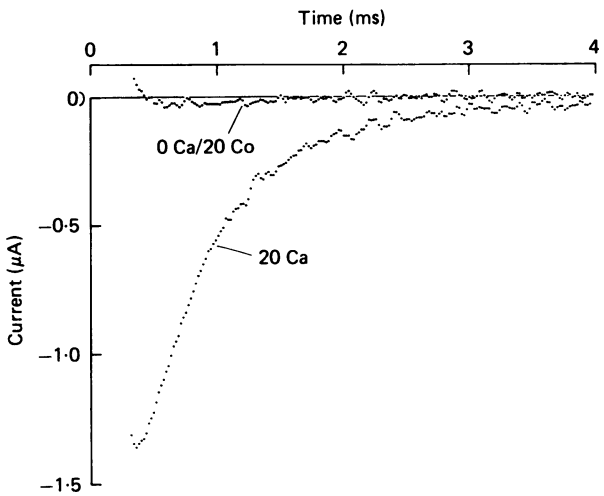

Fig. 2. Tail current eliminated by calcium-blocking agent. Tail current was recorded in 20 mM-calcium artificial sea water (20 Ca) at the end of a 7 ms pulse to +40 mV. Replacing the calcium with cobalt (0 Ca/20 Co) abolished the current.

The corrected tail currents ($d+h$) were routinely displayed on semilogarithmic coordinates (Fig. 1*D*). Within the time frame of our measurements (extending to 10 ms after pulse end), two exponential components were evident: a slow component decaying with a time constant, τ_2, of $2{\cdot}0 \pm 0{\cdot}8$ ms (S.D., $n = 16$), and a fast component decaying with a time constant, τ_1, of $0{\cdot}38 \pm 0{\cdot}05$ ms (S.D., $n = 16$). At 400 μs the fast component has an amplitude (after subtraction of τ_2) that is about an order of magnitude larger than the slow one. At shorter times the ratio of the two amplitudes should be larger. The values for τ_1 reported before our computerized analyses (Eckert & Ewald, 1981) were based on graphic measurements that yielded excessively high values.

Replacing extracellular calcium with cobalt eliminated both components of the tail current (Fig. 2). Manganese was somewhat less effective than cobalt in blocking the tail current, leaving up to 10% of the amplitude obtained in calcium artifical sea water. There was no clear indication of an asymmetric current after the ionic current was blocked, which agrees with the findings of Byerly & Hagiwara (1982), but differs with a report by Kostyuk, Krishtal & Pidoplichko (1981) that 30% of the tail current amplitude recorded in dialysed neurones of *Helix* represents an asymmetric gating current. One possible cause for this difference in behaviour is that the low temperature (i.e. 9 °C) used by Kostyuk *et al.* favours the gating current over the ionic current,

the latter having the higher Q_{10}. Large gating current relative to ionic current in perfused neurones may also indicate that a large proportion of the current is blocked as a result of time-dependent 'wash-out' of the calcium current (Byerly & Hagiwara, 1982). It is also possible that the gating process is blocked by cobalt ions. Absence of a detectable gating current attributable to sodium channels may be accounted for by the loss of much of the sodium current after axotomy was performed.

Tail current amplitude depended on test pulse duration (Fig. 3*A*). The τ_1 and τ_2 components both rose to a maximum within about 20 ms and then underwent similar decreases in amplitude as test pulse durations were further increased (Fig. 3*B*). A plot of the two components against time exhibited a time course of decay approximating the sum of two exponentials with time constants of about 75 and 550 ms, respectively. These are similar to the time constants of two phases of inactivation of the calcium current during a prolonged pulse (Chad, Eckert & Ewald, 1984).

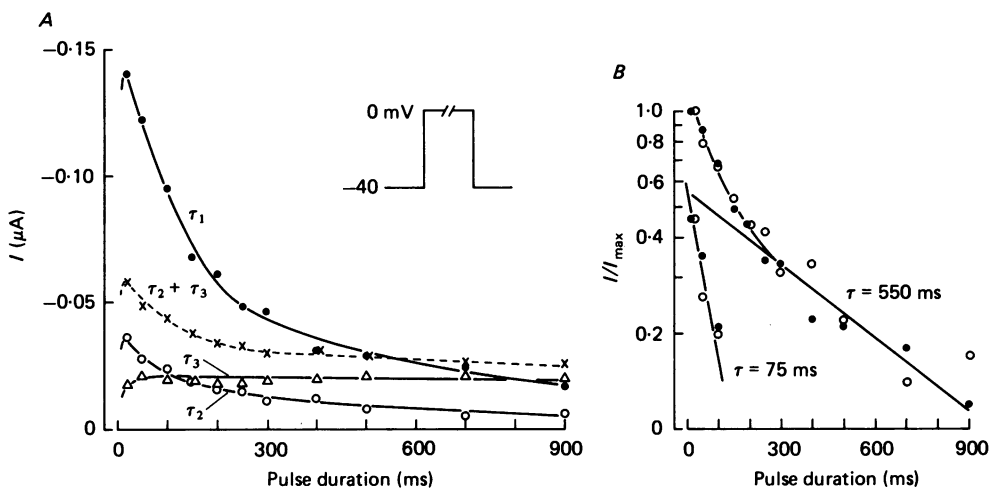

Fig. 3. Amplitude of three components of the tail current plotted against the test pulse duration. *A*, amplitudes at 400 μs after the end of the pulse were determined by computer-assisted fitting of the tail currents to two exponentials ($\tau_1 = 0{\cdot}40$ ms and $\tau_2 = 2{\cdot}4$ ms). The time constant of decay of τ_3 was too long (≈ 30 ms) to affect the measurement of τ_1 and τ_2. *B*, semilogarithmic plots of the normalized amplitudes of the τ_1 (●) and τ_2 (○) components against test pulse duration.

In addition to components τ_1 and τ_2, there can be a third, slower inward tail current. This current has a time constant of decay, τ_3, of the order of 30 ms, and was generally not resolved in the 10 ms recordings following 7 ms test pulses. It differs from τ_1 and τ_2 in developing more slowly as a function of increasing pulse duration, and in failing to undergo subsequent reduction, as do τ_1 and τ_2, with increase in test pulse duration (triangles in Fig. 3*A*). When the τ_2 and τ_3 components are added together (dashed plot, Fig. 3*A*) the summed amplitude of the two components decreases with increased pulse duration along a time course resembling that of the 'slow tail current' described by Byerly & Hagiwara (1982).

Current–voltage relations

Current–voltage relations, obtained with depolarizing pulses to potentials up to +120 mV, are plotted in Fig. 4 as amplitudes of tail currents, I_{tail}, and components τ_1 and τ_2, plus the net current measured just before the end of the pulse (I_{pulse}). The latter is evidently contaminated by outward current during depolarizations exceeding about 0 mV. Above +50 mV the outward current exceeds the calcium current and the mixed current becomes net outward. The outward current is attributed in part to an incomplete blockage of potassium currents, which undergo increasing activation with increased positive potential (Hermann & Gorman, 1979), and in part to the so-called non-specific current (Kostyuk, Krishtal & Shakhovalov, 1977; Byerly & Hagiwara, 1982).

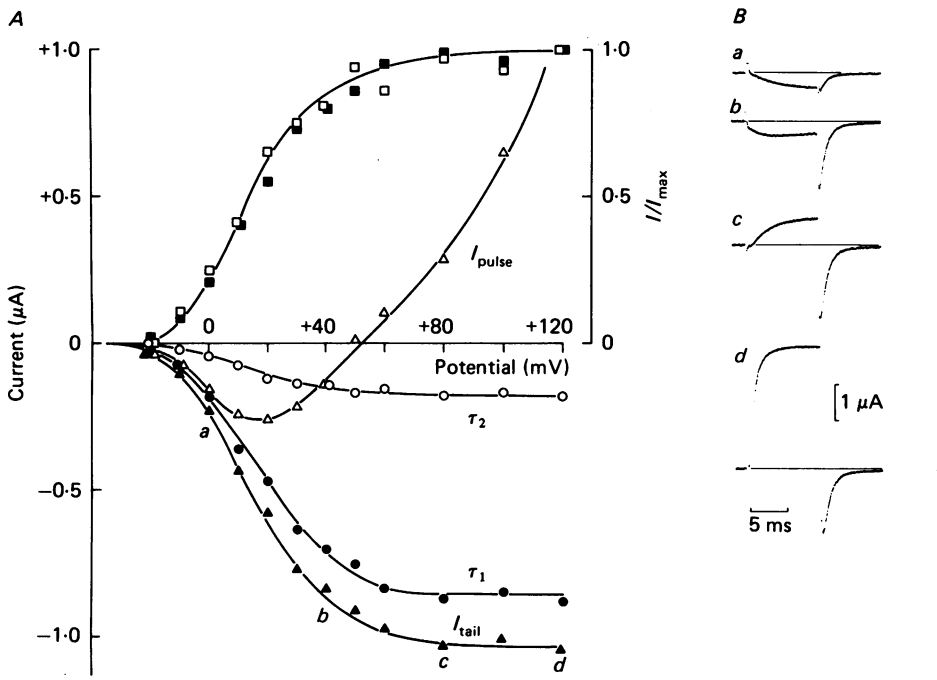

Fig. 4. Current–voltage relations. *A*, I_{pulse}, the current measured just before the end of the 10 ms test pulse, crosses the voltage axis at about +50 mV, indicating that the inward current during depolarizations above 0 mV is contaminated by outward current. In contrast, the two components of the tail current, τ_1 and τ_2, measured 400 μs after the end of the pulse, exhibit sigmoidal increase. The normalized amplitudes of τ_1 (■) and τ_2 (□) components exhibit similar current–voltage relations. *B*, sample traces at selected potentials (*a–d*) indicated in *A*. The hook-like distortion due to inadequate voltage control increased with pulse amplitude, producing a decrease in over-all amplitude of the current tail in record *d* in which the pulse was to +120 mV. The measurement of amplitude in *d* made by extrapolation back to 400 μs from the first exponential portion of the tail.

In contrast to the current recorded during the test pulse, the tail current and its constituent components τ_1 and τ_2 exhibited sigmoidal relations to the voltage during the test pulse, with a plateau above about +80 mV. For potentials up to +100 mV the tail current shows little degradation that might be ascribed to a contaminating outward current. This suggests that the calcium tail currents routinely measured

following much smaller activation of outward current during relatively small depolarizations (to +20 mV or less in most of the remaining experiments) were essentially free from contamination.

Relative amplitude, I/I_{max}, plotted against test pulse potential (square symbols in Fig. 4*A*) is seen to increase similarly with increased voltage for both the τ_1 and τ_2 components. Both components of the tail current thus appear to arise from a single set of channels or from two sets having identical macroscopic conductance–voltage characteristics.

Temporal characteristics of the tail current

The kinetics and amplitudes of the tail currents were sensitive to temperature, the time constant τ_1 exhibiting a Q_{10} of −1·5 between 10 and 20 °C (Fig. 5). The amplitude of the current described by τ_1 exhibited a Q_{10} of 2·2 between 10 and 20 °C. Dependence of tail current kinetics on membrane potential was determined by clamping back to

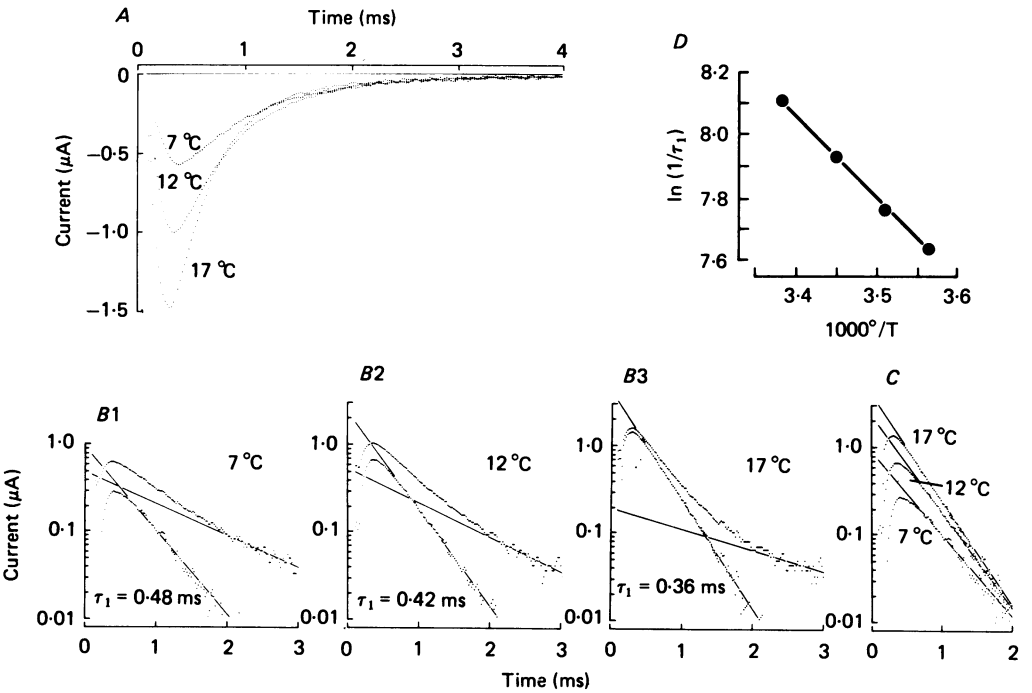

Fig. 5. Temperature dependence of tail currents. *A*, net tail currents following a 7 ms pulse to +20 mV at three temperatures. *B*1–*B*3, semilogarithmic displays of those currents. *C*, comparison of the τ_1 components. *D*, Arrhenius plot of τ_1 against temperature.

different potentials following 7 ms test pulses to +20 mV (Fig. 6). The time constant τ_1 decreased with increased negative potential, but τ_2 showed little change with altered membrane potential. Since an increase in negative potential or an increase in temperature both decreased τ_1, frequency limitations inherent in the recording method may have prevented full resolution of the maximum rate of tail current decay. The Q_{10} and voltage dependency should therefore be taken as lower-limit values.

The entry and accumulation of calcium ions has been implicated in the inactivation of the calcium current (Brehm & Eckert, 1978; Tillotson, 1979; Eckert & Tillotson,

1981; Plant & Standen, 1981). It is possible that entry of calcium during the test pulse and during the tail current may affect the kinetics of the tail current. Several tests were applied to determine whether a change in the internal concentration of calcium ions produces a measurable change in the kinetics of the tail current. Pressure injection of calcium ions into the soma (Eckert & Ewald, 1983) caused partial inactivation of the calcium conductance, seen as a reduction in tail current amplitude to less than 60 % of control. This reduction in amplitude was unaccompanied by any detectable change in kinetics of the tail current.

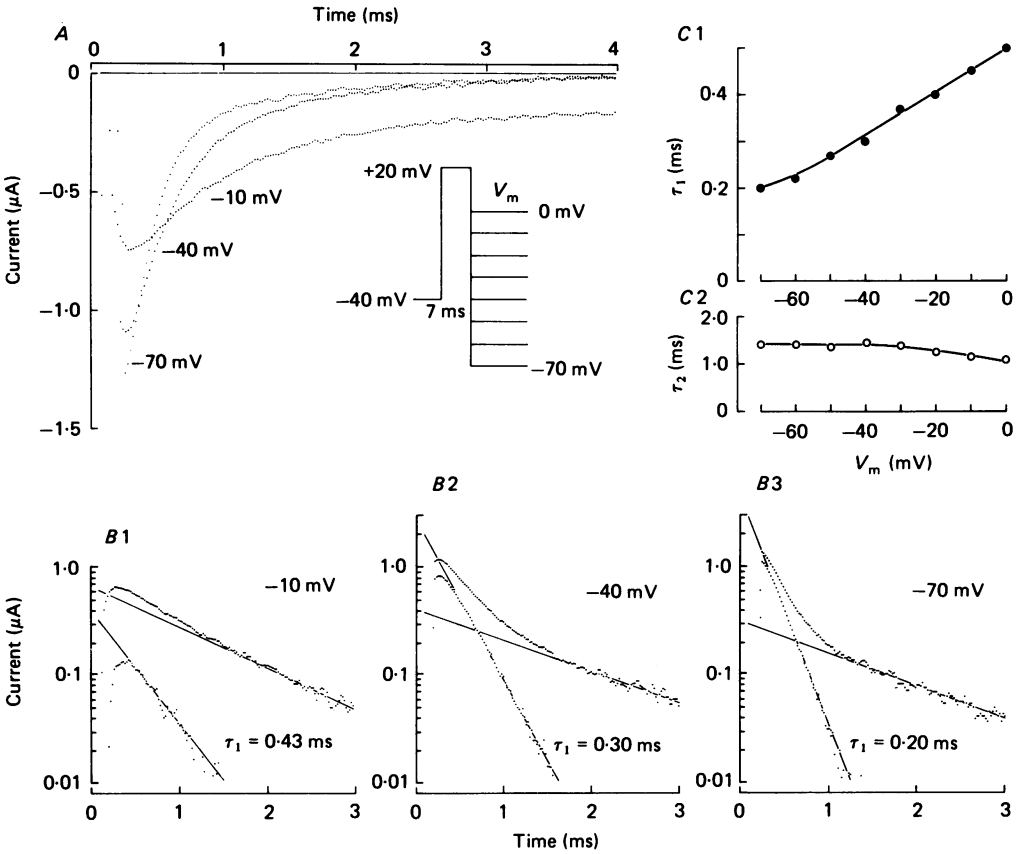

Fig. 6. Potential dependence of deactivation kinetics. *A*, test pulse was followed by membrane potential, V_m, set to different levels. Note that current does not return to zero when $V_m = -10$ mV. *B1–B3*, semilogarithmic displays of the currents. *C1–C2*, τ_1 and τ_2 plotted against membrane potential. Zero was taken as the current level 10 ms after the end of the pulse.

In other experiments, sufficient EGTA was injected to block all but a trace of calcium-dependent inactivation remaining 1000 ms after a 200 ms conditioning depolarization to +10 mV. The injection of EGTA produced no measured changes in the time constants τ_1 and τ_2, although the amplitude of both components, along with a calcium current during the test pulse, increased following injection of EGTA.

If calcium entry during the tail current itself had a measurable effect on the rate

of deactivation, we would expect to see differences in kinetics for tail currents of different amplitudes; however, no changes in the time constants were found with changes in current amplitude (Fig. 7). However, it is possible that the early part of the tail current (i.e. < 400 μs), which is lost under our recording conditions, would show a calcium-dependent effect if it could be resolved.

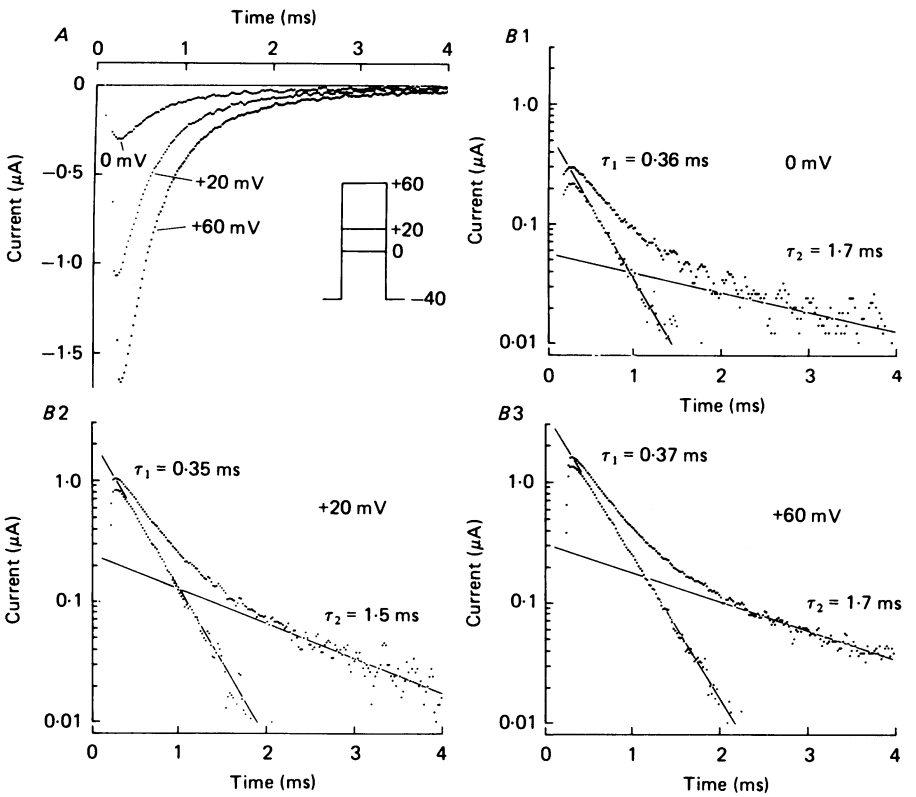

Fig. 7. Pulse amplitude and tail current kinetics. *A*, currents following 7 ms pulses to three different membrane potentials. *B*1–*B*3, semilogarithmic displays of the currents. No significant difference was seen in time constants of the fast and slow components.

The time course of the τ_1 component of the tail current was compared at several membrane potentials with the time course of activation at similar potentials (Fig. 8). The true time course of activation is undoubtedly obscured by the development of some calcium-mediated inactivation during the activation phase, which should diminish the amplitude and advance in time the inward current peak (Chad *et al.* 1984). The rate of activation may therefore be slightly underestimated in these measurements.

The Hodgkin–Huxley (1952*b*) model for the sodium current predicts that if the voltage-dependent time constant for activation is τ_m, the voltage-dependent time constant for deactivation should be $\tau_m/3$. While the time constant of deactivation of the sodium current in squid giant axon appears to agree with that predicted from the kinetics of activation, a similar correspondence appears not to be the case for the

activation and deactivation of calcium currents in snail neurones (Kostyuk, Krishtal & Pidoplichko, 1981; Byerly & Hagiwara, 1982); τ_1 of the calcium tail current in snail neurones is reported to be three to seven times (depending on voltage) as fast as the τ_m for activation of the current. Assuming m^2 activation kinetics, the τ_m for the activation at a given membrane potential can be determined as equal to $T_a/1{\cdot}23$, where T_a is the time to half-amplitude of the peak current (Byerly & Hagiwara, 1982).

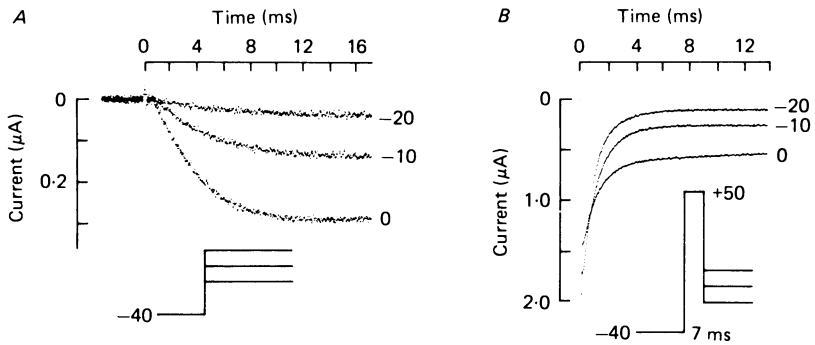

Fig. 8. Comparison of time courses of activation and deactivation of calcium current at three potentials. *A*, activation at −20, −10 and 0 mV. Times to half-peak amplitude (T_a) were 4·4, 3·4 and 3·1 ms, respectively. *B*, deactivation tail currents in same cell at −20, −10 and 0 mV following a 7 ms pulse to +50 mV. Values for τ_1 at these potentials were 0·50, 0·61 and 0·73 ms, respectively. Value of τ_1 at −40 mV was 0·36 ms.

In our experiments, done at 13 °C, the values of τ_m determined from the activation times were two to three times longer than those obtained at 23–27 °C for *Helix* (Byerly & Hagiwara, 1982). Thus, the τ_m values determined from data shown in part in Fig. 8 were 3·6 ms at −20 mV, 2·8 ms at −10 mV, and 2·5 ms at 0 mV. These values are similar to, but slightly lower than, values obtained from model fits to recorded currents (Chad *et al.* 1984). The difference can be attributed to a systematic underestimation of time to peak activation. The underestimation of time to peak occurs because inactivation developing during activation causes the current to peak before activation is complete. As in *Helix*, the τ_m calculated from τ_1 of the tail current was significantly shorter than the τ_m determined from T_a. The value τ_1 was 0·36 ms at −40 mV, 0·50 ms at −20 mV, 0·61 ms at −10 mV and 0·73 ms at 0 mV. For tail currents decaying to a state of full deactivation (i.e. all channels shut) from a state of full activation (i.e. essentially all channels open) the Hodgkin–Huxley formulation predicts that $\tau_1 = 0{\cdot}5\ \tau_m$. These conditions are approximated for the −20 mV tail current, yielding a predicted τ_m of 1·0 ms. As noted above, the τ_m of activation, determined from T_a, was 3·6 ms at this potential. For similar determinations on *Helix* neurones at −30 mV, Byerly & Hagiwara (1982) found a ratio of 7·3 between the predicted and actual rate of deactivation. Extrapolating to the same voltage, we obtain a ratio of 5·8. At higher potentials a substantial proportion of the channels remain open, so that at 0 mV τ_1 is predicted to approximate τ_m. Here the ratio of predicted to actual τ_1 is 3·3, which is identical to that found by Byerly & Hagiwara (1982) at 0 mV.

DISCUSSION

The results of these experiments demonstrate that calcium tail currents can be measured in intact *Aplysia* neurones with minimal disturbance of cell function by voltage clamping at reduced temperature using micro-electrodes of sufficiently low resistance. However, the frequency limitations inherent in this method prevent measurement during the initial 400 μs following the end of the test pulse. Several lines of evidence indicate that the tail currents measured in the presence of TTX and TEA result from ionic current flowing through the deactivating calcium channels. The current is blocked by cobalt and manganese (Fig. 5). Its amplitude and kinetics are sensitive to temperature (Fig. 4) and membrane potential (Fig. 6). The amplitude of the tail current, but not its kinetics, depends on the membrane potential during the test pulse (Fig. 7), plateauing above about +60 mV (Fig. 4). The amplitude of the tail current is independent of the size or direction of the net ionic current recorded before the end of the test pulse (Fig. 4). The tail current amplitude taken at different times after the onset of depolarization has an envelope similar to the time course of the prolonged calcium current (Fig. 3; Chad *et al.* 1984).

The tail current kinetics can, in principle, be influenced by two primary events that accompany the sudden repolarization of the membrane. First, there is the statistical deactivation of the calcium channel population due to removal of voltage-dependent activation. Secondly, the repolarization, by increasing the driving force on calcium ions (i.e. the membrane potential minus the calcium equilibrium potential), causes a transient increase in the rate of entry of calcium and a momentary increase in the activity of calcium near the inner surface of the membrane. The increase in calcium concentration should cause a sudden increase in calcium-mediated inactivation of calcium channels (Brehm & Eckert, 1978; Tillotson, 1979; Eckert & Tillotson, 1981). While this process may play a role, our results provide no measurable indication that calcium-mediated inactivation affected the kinetics of the tail currents. Changing the amplitude of the tail current, and hence the surge of calcium ions, by varying the potential of (and thus the percentage of calcium channels activated during) the test pulse produced no measured change in time constants (Fig. 7); neither did injection of EGTA produce a significant change in the time constants. Thus, within the limitations of our resolution, the kinetics of the tail currents appear to be determined primarily by voltage-dependent deactivation, with little or no contribution from calcium-dependent inactivation.

The tail current contains two phases of relaxation, τ_1 and τ_2, exhibiting time constants of about 0·38 and 2·0 ms, respectively, at 12–14 °C. With pulse durations of 10 ms or longer, a slow third component, τ_3, became apparent. This component is characterized by a slower time course of development, a rate of decay an order of magnitude slower than τ_2 and little or no loss of amplitude (i.e. no inactivation) with increasing pulse duration (Fig. 3). The slow-non-inactivating third component appears to be unrelated to the calcium current, and may instead be related to the non-specific current described in snail neurones (Kostyuk *et al.* 1977; Byerly & Hagiwara, 1982) and recently attributed to an efflux of protons through calcium-sensitive channels activated at potentials in excess of 0 mV (Thomas & Meech, 1982). The sum of the second and third components (Fig. 3*A*) behaves somewhat like the

'slow tail current' reported in measurements made on perfused *Limnaea* neurones (Byerly & Hagiwara, 1982).

The τ_1 and τ_2 components we measured both show similar current–voltage relations (Fig. 4), kinetics that are independent of test pulse potential or calcium entry (Fig. 7), and both are blocked by cobalt substitution for calcium in the bath. Both components undergo a proportional loss of amplitude (i.e. inactivation) with prolonged pulse duration (Fig. 3), the amplitudes declining with a two-component time course similar to that which characterizes the decay of the calcium current during a sustained depolarization (Chad *et al.* 1984). On the other hand, time constants τ_1 and τ_2 differ in temperature sensitivity (Fig. 5) and voltage sensitivity (Fig. 6), τ_2 exhibiting little sensitivity to either temperature or voltage.

The first and second components of the calcium tail current might represent (i) the closing of two differing populations of calcium channels, or (ii) the kinetics of multistate transitions from open to closed states within a homogeneous population of channels. We favour the second interpretation, which is embodied in a computer model of the calcium channel which includes m^2 voltage-dependent activation and inactivation proportional to intracellular free calcium ions (Eckert, Ewald & Chad, 1982; Chad *et al.* 1983, 1984). This model, similar to that proposed by Standen & Stanfield (1982) and by Plant, Standen & Ward (1983), assumes a uniform population of channels, accurately simulates the inactivation of the calcium current, and also predicts a tail current with two time constants. The first phase of the tail current in the model is dependent on inactivation caused by the surge of calcium ions entering upon repolarization following brief depolarizations. Failure of τ_1 in our experiments to exhibit any dependence on the rate of calcium entry (Fig. 7) suggests that the two time constants may represent two states of deactivation. This suggests that the m^2 formulation for activation used in the models (Eckert *et al.* 1982; Plant *et al.* 1983) may be an oversimplification, a conclusion also supported by the discrepancy noted earlier between the time constants of activation and the time constants of deactivation predicted by the m^2 formulation.

Two components of calcium tail currents have been reported for neurones of *Helix* (Tsuda, Wilson & Brown, 1982) and *Limnaea* (Byerly & Hagiwara, 1982) as determined in dialysed cells. The τ_1 values reported for dialysed snail neurones were 0·1–0·2 ms and the τ_2 values were 1·2–1·5 ms. These τ_1 values are about three times as fast as the values we found for *Aplysia* neurones, and the τ_2 values about twice as fast. Byerly & Hagiwara (1982) suggest that the true time constant of the first phase of the tail current may in fact be shorter than their shortest measured time constants of about 100 μs, which may be slowed due to frequency limitations of the clamp. Differences between the time constants measured in snail neurones and those reported above for *Aplysia* could represent true differences in channel kinetics due to different species characteristics and/or differences in working temperatures (13 °C for *Aplysia*, 23–27 °C for *Limnaea*), or they could result from differences in the speed and uniformity of voltage control during repolarizing steps. Although some loss in high frequency is likely in our measurements, the differences in rates appear to result primarily from true differences in kinetics, for we see an approximately proportional slowing of both fast and slow components in our measurements compared with those of Byerly & Hagiwara (1982) in *Limnaea*. Thus, the ratios of time constant τ_1 to τ_2

and of τ_1 to T_a in the *Aplysia* measurements are similar to the corresponding ratios seen in *Helix*. Frequency-limited slowing of the current recordings would act preferentially on the faster components and should diminish these ratios. The rates measured in *Aplysia* at 13 °C are 2·5–3·5 times slower than those measured in *Limnaea* at 23 °C. This is in the range expected for temperature-dependent slowing of channel kinetics; thus the relatively slow temporal characteristics of our currents do not appear to result from any fundamental differences in channel kinetics between *Aplysia* neurones and snail neurones.

We acknowledge the invaluable discussions, suggestions and comments of Drs J. Chad, G. Augustine and J. Deitmer, and also J. Cowman's assistance. We are especially indebted to Dr Chad for his supervision of the computer analyses. The work was supported by USPHS NS8364, NSF BNS 80-12346 and the Epilepsy Foundation of America.

REFERENCES

ASHCROFT, F. M. & STANFIELD, P. R. (1981). Calcium dependence of the inactivation of calcium currents in skeletal muscle fibers of an insect. *Science, N.Y.* **213**, 224–226.

ASHCROFT, F. M. & STANFIELD, P. R. (1982). Calcium and potassium currents in muscle fibres of an insect (*Carausius morosus*). *J. Physiol.* **323**, 93–115.

BREHM, P. & ECKERT, R. (1978). Calcium entry leads to inactivation of calcium channel in *Paramecium*. *Science, N.Y.* **202**, 1203–1206.

BYERLY, L. & HAGIWARA, S. (1982). Calcium currents in internally perfused nerve cell bodies of *Limnea stagnalis*. *J. Physiol.* **322**, 503–528.

CHAD, J., ECKERT, R. & EWALD, D. (1983). Kinetics of calcium current inactivation simulated with a heuristic model. *Biophys. J.* **41**, 61a.

CHAD, J., ECKERT, R. & EWALD, D. (1984). Kinetics of calcium-dependent inactivation of calcium current in voltage-clamped neurones of *Aplysia californica*. *J. Physiol.* (in the Press).

CONNOR, J. A. & STEVENS, C. F. (1971). Voltage clamp studies of a transient outward membrane current in gastropod neural somata. *J. Physiol.* **213**, 21–30.

ECKERT, R. (1981). Calcium-mediated inactivation of voltage-gated Ca channels. In *The Mechanism of Gated Calcium Transport Across Biological Membranes*, ed. OHNISHI, S. T. & ENDO, M. New York: Academic Press.

ECKERT, R. & EWALD, D. (1981). Ca-mediated Ca channel inactivation determined from tail current measurements. *Biophys. J.* **33**, 145a.

ECKERT, R. & EWALD, D. (1982). Ca-dependent inactivation of Ca conductance in *Aplysia* neurons exhibits voltage dependence. *Biophys. J.* **37**, 182a.

ECKERT, R. & EWALD, D. (1983). Inactivation of calcium conductance characterized by tail current measurements in neurones of *Aplysia californica*. *J. Physiol.* **345**, 549–565.

ECKERT, R., EWALD, D. & CHAD, J. (1982). A single calcium-mediated process can account for both rapid and slow phases of inactivation exhibited by a single calcium conductance. *Biol. Bull.* **163**, 398.

ECKERT, R. & TILLOTSON, D. (1981). Calcium-mediated inactivation of the calcium conductance in caesium-loaded giant neurones of *Aplysia californica*. *J. Physiol.* **314**, 265–280.

ECKERT, R., TILLOTSON, D. & BREHM, P. (1981). Calcium mediated control of Ca and K currents. *Fedn Proc.* **40**, 2226–2232.

HAGIWARA, S. & BYERLY, L. (1981). Calcium channel. *A. Rev. Neurosci.* **4**, 69–125.

HAGIWARA, S. & SAITO, N. (1959). Voltage–current relations in nerve cell membrane of *Onchidium verruculatum*. *J. Physiol.* **148**, 161–179.

HERMANN, A. & GORMAN, A. L. F. (1979). External and internal effects of tetraethylammonium on voltage-dependent and Ca-dependent K^+ current components in molluscan pacemaker neurons. *Neurosci. Lett.* **12**, 87–92.

HERMANN, A. & GORMAN, A. L. F. (1981*a*). Effects of 4-aminopyridine on potassium currents in a molluscan neuron. *J. gen. Physiol.* **78**, 63–86.

HERMANN, A. & GORMAN, A. L. F. (1981*b*). Effects of tetraethylammonium on potassium currents in a molluscan neuron. *J. gen. Physiol.* **78**, 87–110.

HODGKIN, A. L. & HUXLEY, A. F. (1952*a*). The dual effect of membrane potential on sodium conductance of the giant axon of *Loligo*. *J. Physiol.* **116**, 497–506.

HODGKIN, A. L. & HUXLEY, A. F. (1952*b*). A quantitative description of membrane current and its application to conduction and excitation in nerve. *J. Physiol.* **117**, 500–544.

KOSTYUK, P. G., KRISHTAL, O. A. & PIDOPLICHKO, V. I. (1975). Effect of internal fluoride and phosphate on membrane currents during intracellular dialysis of nerve cells. *Nature, Lond.* **257**, 691–693.

KOSTYUK, P. G., KRISHTAL, O. A. & PIDOPLICHKO, V. I. (1981). Calcium inward current and related charge movements in the membrane of snail neurones. *J. Physiol.* **310**, 403–421.

KOSTYUK, P. G., KRISHTAL, O. A. & SHAKHOVALOV, Y. A. (1977). Separation of sodium and calcium currents in the somatic membrane of mollusc neurones. *J. Physiol.* **270**, 545–568.

LEE, K. S., AKAIKE, N. & BROWN, A. M. (1978). Properties of internally perfused, voltage-clamped, isolated nerve cell bodies. *J. gen. Physiol.* **71**, 489–507.

PLANT, T. D. & STANDEN, N. B. (1981). Calcium current inactivation in identified neurones of *Helix aspersa*. *J. Physiol.* **321**, 273–285.

PLANT, T. D., STANDEN, N. B. & WARD, T. A. (1983). The effects of injection of calcium ions and calcium chelators on calcium channel inactivation in *Helix* neurones. *J. Physiol.* **334**, 189–212.

STANDEN, N. B. & STANFIELD, P. R. (1982). A binding-site model for calcium channel inactivation that depends on calcium entry. *Proc. R. Soc.* B **217**, 101–110.

THOMAS, R. C. & MEECH, R. W. (1982). Hydrogen ion currents and intracellular pH in depolarized voltage-clamped snail neurones. *Nature, Lond.* **299**, 826–828.

TILLOTSON, D. (1979). Inactivation of Ca conductance dependent on entry of Ca ions in molluscan neurons. *Proc. natn. Acad. Sci. U.S.A.* **77**, 1497–1500.

TSUDA, Y., WILSON, D. L. & BROWN, A. M. (1982). Calcium tail currents in snail neurons. *Biophys. J.* **37**, 181a.

ZUCKER, R. (1981). Tetraethylammonium contains an impurity which alkalizes cytoplasm and reduces calcium buffering in neurons. *Brain Res.* **208**, 473–478.